PHYSICAL REVIEW B **83**, 041403(R) (2011)

Formation of hydrogenated graphene nanoripples by strain engineering and directed surface self-assembly

Z. F. Wang, Yu Zhang, and Feng Liu*

Department of Materials Science and Engineering, University of Utah, Salt Lake City, Utah 84112, USA

(Received 23 November 2010; published 14 January 2011)

We propose a class of semiconducting graphene-based nanostructures: hydrogenated graphene nanoripples (HGNRs), based on continuum-mechanics analysis and first-principles calculations. They are formed via a two-step combinatorial approach: first by strain-engineered pattern formation of graphene nanoripples, followed by a curvature-directed self-assembly of H adsorption. It offers a high level of control of the structure and morphology of the HGNRs, and hence of their band gaps, which share common features with graphene nanoribbons. A cycle of H adsorption (desorption) at (from) the same surface locations completes a reversible metal-semiconductor-metal transition with the same band gap.

DOI: 10.1103/PhysRevB.83.041403 PACS number(s): 61.48.Gh, 62.25.−g, 68.43.−h, 81.05.ue

Nanostructures have distinct properties from their bulk counterparts. In the case of graphene, nanostructuring affords an effective means to convert the semimetal graphene[1] into semiconducting graphene based nanostructures, which is desirable for many nanoelectronics applications.[2] A number of theoretical proposals and experimental attempts have been made to create graphene-based nanostructures, such as graphene nanoribbons,[3–7] nanohole superlattices,[8–10] hydrogenated graphene nanostripes,[11–13] and graphane.[14] However, our current success is still far below our expectations. Although the physical principles for opening the graphene band gap are well established, the synthesis of the semiconducting graphene-based nanostructures with desirable precision and control remains challenging. Lithographic patterning of graphene into nanodimensions has difficulties in controlling the nanopattern size and edge qualities. The method using H adsorption on graphene is fundamentally a stochastic process, and the means for directing H to the exact locations as needed is not established.

In this paper, we propose a strain-engineered self-assembly process to form a class of graphene-based nanostructures, the hydrogenated graphene nanoripples (HGNRs). The process consists of two steps: first, strain engineering graphene into periodic nanoripple patterns, followed by a directed self-assembly of H adsorption onto the nanoripple template. The combination of the strain engineering and the directed H surface self-assembly offers a high level of control of the dimensions of the HGNRs and hence of their band gaps, which share common scaling features with graphene nanoribbons.

Generally, two physical mechanisms have been employed for opening the band gap in graphene. One is by imposing the quantum confinement effect. The semimetal behavior of graphene stems from the free motion of two-dimensional (2D) π electrons. If the motion of π electrons is confined, then the band gap opens. This can be achieved by cutting graphene into nanoribbons[3–6] and nanonetworks,[8–10] or by H adsorption[11–13] where locally π bands are removed due to the change from sp^2 to sp^3 hybridization. The other mechanism is by breaking the graphene lattice symmetry. In the pristine graphene, the π bands, residing on the A sublattice, are degenerate with the π^* bands, residing on the B sublattice, at Fermi energy. If such symmetry is broken,[15] then gap opens. This has been shown in the spin-polarized graphene zigzag edges[4,5,11,12] and in the epitaxial graphene grown on compound BN (Ref. 16) and SiC (Ref. 17) substrates, where spin and substrate potential lifts the energy degeneracy between the π and π^* bands, respectively.

To implement the aforementioned mechanisms, the basic idea of our combinatorial approach of strain engineering and directed surface self-assembly is illustrated in Fig. 1. Starting with a pristine graphene sheet of length L [Fig. 1(a)], in the first step of "strain engineering," a compressive strain (ε) is applied along L to form a one-dimensional (1D) pattern of graphene nanoripple with period N_W [Fig. 1(b)] [N_W is the number of dimer and zigzag lines denoting the width of armchair and zigzag nanoripples, respectively; see Figs. 3(a) and 3(d)]. At this step, the nanoripple remains a semimetal. In the second step of "chemical engineering," H atoms are introduced to adsorb onto the ripple pattern at designated locations [Fig. 1(c)] to form the HGNRs. Now, the band gap opens. The nanoripple formation in the first step has two key functions. First, its period defines the period of the HGNR (i.e., the width of the hydrogenated nanostripes created in the second step, and hence the eventual size of the band gap). Second, its morphology serves as a template to direct H atoms to be adsorbed at specific locations with the largest local curvature, so as to form highly ordered H patterns. The directed H adsorption in the second step fulfills the role of opening a predefined band gap.

There are several noteworthy advantages of the foregoing approach. The band gap as engineered is tunable with a high level of control. It is well known that the band gap scales inversely with graphene nanoribbon widths.[3–6] Here, the width of the HGNR is uniquely defined by the period of the nanoripple without H adsorption, which can be tuned precisely by the magnitude of the compressive strain applied and the length of graphene used. Because the H atoms are directed by the nanoripple template to the designated locations of the largest curvature, instead of random adsorption sites, they form a highly regular pattern, which translates the HGNR into an ordered array of graphene nanostripes with the highly uniform width, orientation, and smooth edges, so that they all open a predefined uniform band gap. Furthermore, the approach makes a repeatable process, as a cycle of the directed H adsorption and desorption leads naturally to a cycle of metal-semiconductor-metal transition opening the

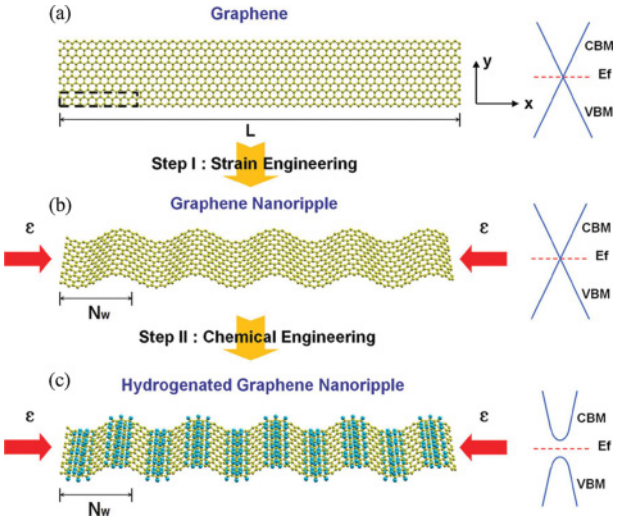

FIG. 1. (Color online) Schematic illustration of a combinatorial approach of straining graphene and directing H adsorption to form HGNR. (a) Pristine graphene with zero band gap. L denotes the length. Dashed line shows the unit cell. (b) Graphene nanoripple with zero band gap. ε and N_W denote the compressive strain and the ripple period, respectively. (c) HGNR with nonzero band gap. E_f is the Fermi energy; CBM (VBM) is the conduction (valence) band minimum (maximum).

same band gap in the HGNR. In the following, we discuss the processing parameters of the HGNRs and their resulting electronic properties.

We first analyze the strain-induced nanoripple pattern formation in graphene, based on a continuum mechanics model.[18,19] Consider a uniaxial compressive strain ε applied along the x direction [Fig. 1(b)] of a graphene sheet of length L. Above a critical strain value, the flat graphene becomes unstable and undulates into a 1D sinusoidal ripple pattern with period N_W. The total energy of the ripple can be calculated as

$$U_{\text{total}} = U_{\text{bending}} + U_{\text{stretching}} \tag{1}$$
$$= \frac{B}{2}\int\left(\frac{\partial^2\xi}{\partial x^2}\right)^2 dx\,dy + \frac{Eh}{2}\int\varepsilon\left(\frac{\partial\xi}{\partial x}\right)^2 dx\,dy,$$

where B and E are the bending and Young's modulus of graphene, respectively, ξ is the displacement along the z direction, and h is the thickness of graphene. Under the boundary condition $\frac{\partial^2\xi}{\partial x^2}|_{x=0,x=L} = 0$, $\xi(x) = \frac{C}{(n\pi/L)^2}\sin(\frac{n\pi x}{L})$, where n is the number of ripple periods formed and C is a constant. Applying the variational principle, the critical strain for generating the ripple pattern can be obtained as

$$\varepsilon_{\text{cr}} = \frac{Bn^2\pi^2}{EhL^2} = \frac{h^2n^2\pi^2}{12(1-\nu^2)L^2}, \tag{2}$$

where ν is the Poisson ratio.

Figure 2 shows the calculated phase diagram showing the number of ripple periods (n) as a function of strain (ε) and graphene length (L), using $\nu = 0.34$ (Ref. 20) and $h = 0.7$ Å (Ref. 21). For the given L (ε), n increases with increasing $\varepsilon(L)$. Thus, the period of the ripple pattern (N_W) can be tuned by the magnitude of the compressive strain and the length of graphene.

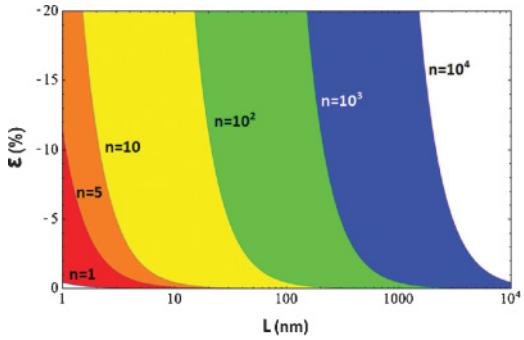

FIG. 2. (Color online) Phase diagram showing the number of ripple periods (n) formed as a function of the graphene length (L) and the applied compressive strain (ε). Boundary lines mark the critical strain (ε_{cr}) in Eq. (2).

Next, we analyze a "directed" H self-assembly on the ripple pattern. The ripple morphology provides a curvature template to direct the H adsorption to the designated locations. To illustrate this effect, we compare the total energies of different hydrogen adsorption configurations by using the first-principles method. The calculations are performed using the VASP package,[22] which implements the local (spin) density approximation[23] of the density functional theory. The electron-ion interaction is described by the projected augmented wave method[24] with an energy cutoff of 400 eV and a k-point mesh of $(15 \times 7 \times 1)$ based on the convergence tests. The atom positions are optimized with the atomic force converged to <0.01 eV/Å.

There are two typical orientations in graphene, the zigzag and armchair directions,[3,4] along which we apply the compressive strain to form the corresponding armchair and zigzag nanoripple, as shown in Figs. 3(a) and 3(d), respectively. For the armchair nanoripple, we choose $N_W = 20$ and $\varepsilon = -10\%$ as an example to demonstrate the directed H adsorption. First, we adsorb two rows of H atoms within one period of the nanoripple to form the armchair HGNR. By comparing the relative adsorption energies per H (setting the most stable adsorption configuration as the zero energy of reference) [Fig. 3(b)], we can see clearly that the H atoms prefer to adsorb onto the carbon atoms with the largest curvature. The H rows divide one ripple period into two equivalent nanostripes of the same width. Next, we absorb another two rows of H atoms, and the stable H adsorption configuration is shown in Fig. 3(c). The additional H rows are attracted to the existing rows, forming two rows of H at the largest curvature locations. Note that the energy difference between the preferred adsorption site and its neighboring sites is relatively small for one row of H [Fig. 3(b)], but this energy difference increases with the increasing H coverage [Figs. 3(c)–3(f)]. This indicates that the H atoms prefer to segregate, forming a strip around the local curvature, as shown in Fig. 1(c), consistent with the H clustering tendency on graphene found earlier.[25] A more direct proof of the curvature-directed H adsorption requires molecular dynamics simulation,[26] which is beyond the scope of our work. Similarly directed H adsorption is also observed in the zigzag HGNR with $N_W = 12$ and $\varepsilon = -10\%$, as shown in Figs. 3(e) and 3(f) for two rows and four rows of H atoms within one period of zigzag nanoripple, respectively.

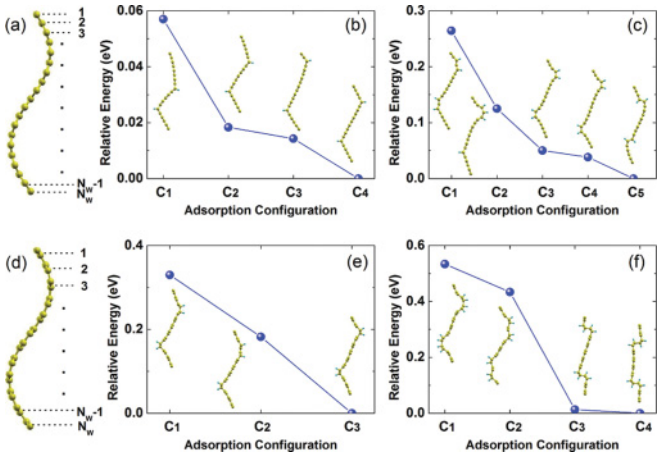

FIG. 3. (Color online) Directed H adsorption onto the graphene nanoripple. (a) and (d) Schematics of one period of armchair and zigzag nanoripple, respectively. N_W denotes the ripple period. (b) and (c) Relative energies of different H adsorption configurations (C_1 through C_5, shown as insets) of armchair HGNR with two and four rows of H atoms within one period of the ripple, respectively. (e) and (f) Same as (b) and (c) for zigzag HGNR. Note that the H row in armchair HGNR is a straight line and the H row in zigzag HGNR is a zigzag line.

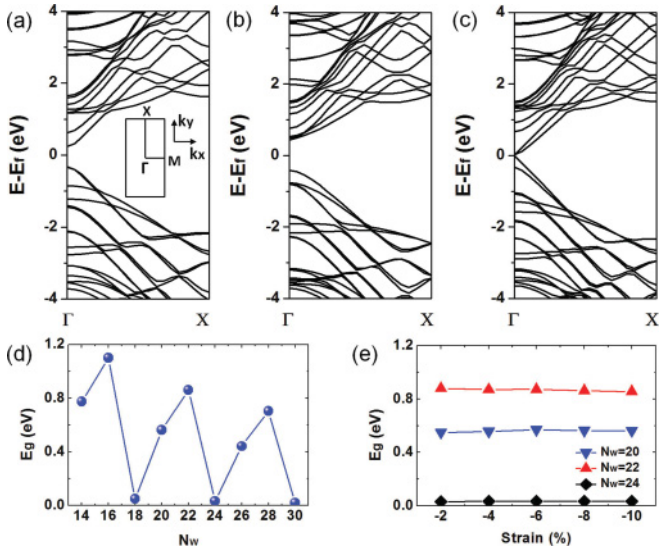

FIG. 4. (Color online) Band structure of the armchair HGNR with two rows of H atoms. (a)–(c) Band structures for $N_W = 20$, 22, and 24 with $\varepsilon = -10\%$, respectively. Inset in (a) shows the first Brillouin zone with three high-symmetry points and the reciprocal coordinate axes. (d) Band gap as a function of N_W for the fixed strain $\varepsilon = -10\%$. (e) Band gap as a function of strain for $N_W = 20$, 22, and 24.

The preferred H adsorption onto the C atoms with the largest curvature is consistent with the previous theoretical[27] and experimental[28] results. This is because, instead of the sp^2 electronic configuration in a planar symmetry, the curved C atom has a $sp^{2+\delta}$ configuration, which is closer to the final sp^3 configuration upon H adsorption.[29] Thus, it costs less energy for H to adsorb onto a curved C atom than onto a planar C atom. Based on the same principle, after H is adsorbed onto a C atom, it makes its neighboring C atoms more like $sp^{2+\delta}$, so that the additional H atoms will prefer to adsorb onto these neighboring C atoms, but on the opposite side of graphene.

Formation of a graphene nanoripple without H does not open the band gap; one role of ripple structure is to provide a template to direct the H adsorption that will open the band gap. Also, the period of the nanoripple patterns defines the period of the HGNR (i.e., the width of nanostripes formed upon H adsorption, and hence of the final band gap). Next, we present the band gaps of the HGNRs as a function of nanoripple period and strain.

In the direction perpendicular to the H row (ΓM direction), the band structures for armchair and zigzag HGNRs are almost flat, so in the following, we only show the band structures along the H row direction (ΓX direction). The band structures of armchair HGNR adsorbed with two rows of H atoms are shown in Fig. 4, similar to those of armchair graphene nanoribbons.[3,4] Figures 4(a)–4(c) are the respective band structures for $N_W = 20$, 22, and 24 with $\varepsilon = -10\%$, in which band gaps can be clearly seen. Without the H, no band gap appears in the armchair nanoripples even when the strain increases to -30%. The physical origin of the band gap is due to quantum confinement. When an H atom is adsorbed onto a C atom, it removes the local π orbital on this C atom, creating a potential barrier blocking the π electrons. Consequently, even one row of H atoms can work as a hard-wall potential to confine the π electrons between H rows to open a band gap. For the fixed strain, the band gap is not a monotonous function of the ripple width, and can be divided into three groups [Fig. 4(d)]. They follow the relation $E_g(N_{W_{\text{eff}}} = 3p + 2) < E_g(N_{W_{\text{eff}}} = 3p) < E_g(N_{W_{\text{eff}}} = 3p + 1)$, which is same as that for the armchair graphene nanoribbons.[4] Here $N_{W_{\text{eff}}} = (N_W - 2)/2$ is the effective nanostripe width and p is a positive integer. For the fixed ripple width, the three band-gap groups show little dependence on the strain [Fig. 4(e)]. Without ripple formation, the band gaps of flat armchair nanoribbons have been shown to depend on in-plane uniaxial strain,[30] because strain changes bond length and hence the interatomic electron hopping energies. With the ripple formation, however, the in-plane strain is largely relaxed by the bending (i.e., change of bond angles) so that the bond length changes very little. This is the reason we see a very weak strain dependence of the band gap in Fig. 4(e). Note that under compressive strain, the ripple structure is usually favored over the planar graphene, because for normal graphene size ($L \sim 10-10^4$nm), the critical strain for ripple formation is extremely small (<0.1%), as shown in Fig. 2.

The band structures of zigzag HGNRs adsorbed with two rows of H atoms are shown in Fig. 5, similar to those of zigzag graphene nanoribbons.[3,4] Figures 5(a)–5(c) show the band structures of the nonmagnetic (NM), ferromagnetic (FM), and antiferromagnetic (AFM) states with $N_W = 12$ and $\varepsilon = -10\%$, respectively. The same pattern holds as for zigzag nanoribbons, in that the zigzag HGNR in Fig. 5 has an AFM ground state, with the NM and FM states being 25.9 meV and 13.8 meV higher in energy, respectively, than the AFM state. The NM state is a metal, with four subbands crossing the Fermi level [Fig. 5(a)]. This is different from the zigzag nanoribbon, which has only two subbands crossing the Fermi level.[4] Because the H atoms divide one ripple period into two nanostripes of the same width, their interaction splits the two subbands into

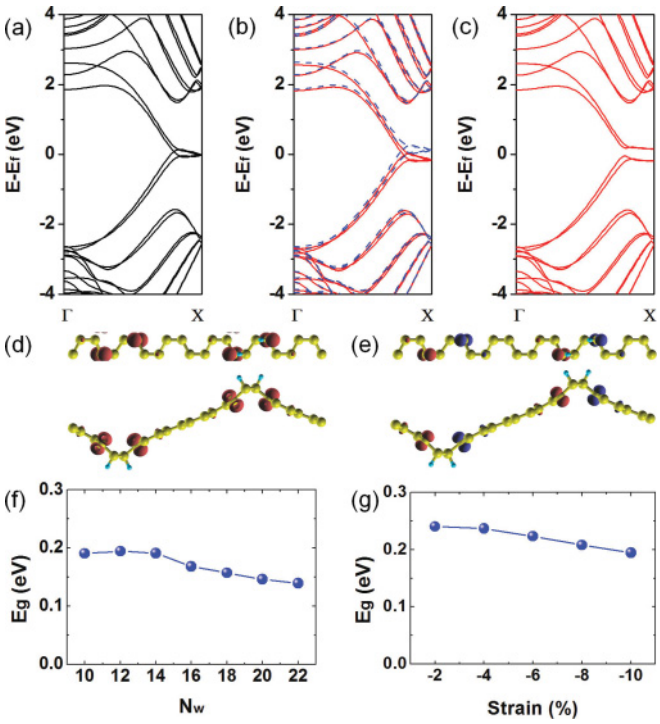

FIG. 5. (Color online) Band structure of the zigzag HGNR with two rows of H atoms. (a)–(c) Band structures for the NM, FM, and AFM states with $N_W = 12$ and $\varepsilon = -10\%$, respectively. The high-symmetry points have the same meaning as those in Fig. 4(a). Red (blue) corresponds to spin-up (spin-down). Spin-up and spin-down are degenerate in (c). (d) and (e) Spatial distribution of spin density ($\rho_{\text{spin-up}} - \rho_{\text{spin-down}}$) for FM (isovalue 0.04) and AFM (isovalue 0.02) states, with $N_W = 12$ and $\varepsilon = -10\%$, respectively. The color has the same spin notion as in (b). (f) Band gap of the AFM state as a function of N_W for the fixed strain $\varepsilon = -10\%$. (g) Band gap of the AFM state as a function of strain for $N_W = 12$.

four. In the transverse direction (ΓM), the flat subbands show similar splitting behavior. With the increasing H convergence, as the two ribbons are separated by wider H rows (i.e., wider and larger potential barriers), we expect the band structure to converge into that of the true nanoribbon without splitting, which is similar to Singh's results.[11] The FM state is a metal, while the AFM state is a semiconductor for both spins. The spatial distribution of spin charge densities is shown in Figs. 5(d) and 5(e) for the FM and AFM states, respectively. For the fixed strain, the band gap of the AFM zigzag HGNR [Fig. 5(f)], opened by the symmetry breaking mechanism, shows a much weaker dependence on the ripple width compared to the band gaps of the armchair HGNR [Fig. 4(d)], opened by the quantum confinement mechanism. For the fixed ripple width, the band gap of the AFM zigzag HGNR [Fig. 5(g)] shows a rather weak dependence on the strain, which is similar to the case of the armchair HGNR [Fig. 4(e)].

In conclusion, we demonstrate theoretically a strain-engineered self-assembly process to fabricate a class of semiconducting graphene-based nanostructures, the HGNRs, which share some common band-gap features of graphene nanoribbons. It is a combinatorial two-step process of straining a graphene sheet into nanoripples followed by the curvature-directed H adsorption, which offers a high level of band-gap control by tuning the magnitude of strain, the dimension of the graphene sheet, and the amount of H adsorption. We note that graphene nanoripples have already been fabricated by straining the suspended graphene sheet experimentally.[31] The prospect of further dosing the nanoripples with H to form the semiconducting HGNRs is very appealing. We expect that the combination of strain-engineered nanoripple formation and the curvature-directed surface self-assembly can be generally applied beyond graphene to other nanomembranes.

This work was supported by DOE-BES (Grant No. DE-FG02-03ER46027) and CMSN program. We thank the Center for High Performance Computing at the University of Utah for providing the computing resources.

*Corresponding author; fliu@eng.utah.edu

[1] K. S. Novoselov *et al.*, Nature (London) **438**, 197 (2005).
[2] Z. F. Wang and F. Liu, ACS Nano **4**, 2459 (2010).
[3] K. Nakada *et al.*, Phys. Rev. B **54**, 17954 (1996).
[4] Y. W. Son, M. L. Cohen, and S. G. Louie, Phys. Rev. Lett. **97**, 216803 (2006).
[5] Q. Yan *et al.*, Nano Lett. **7**, 1469 (2007).
[6] M. Y. Han *et al.*, Phys. Rev. Lett. **98**, 206805 (2007).
[7] X. Li *et al.*, Science **319**, 1229 (2008).
[8] D. Yu *et al.*, Nano Res. **1**, 56 (2008).
[9] W. Liu *et al.*, Phys. Rev. B **80**, 233405 (2009).
[10] J. Bai *et al.*, Nat. Nanotech. **5**, 190 (2010).
[11] A. K. Singh and B. I. Yakobson, Nano Lett. **9**, 1540 (2009).
[12] H. Xiang *et al.*, Nano Lett. **9**, 4025 (2009).
[13] R. Balog *et al.*, Nat. Mater. **9**, 315 (2010).
[14] D. C. Elias *et al.*, Science **323**, 610 (2008).
[15] J. Q. Lu *et al.*, Phys. Rev. Lett. **90**, 156601 (2003).
[16] G. Giovannetti *et al.*, Phys. Rev. B **76**, 073103 (2007).
[17] S. Y. Zhou *et al.*, Nat. Mater. **6**, 770 (2007).
[18] E. Cerda and L. Mahadevan, Phys. Rev. Lett. **90**, 074302 (2003).
[19] Y. Zhang *et al.*, Appl. Phys. Lett. **96**, 111904 (2010).
[20] Z. C. Tu and Z. C. Ou-Yang, Phys. Rev. B **65**, 233407 (2002).
[21] J. Zang, O. Aldás-Palacios, and F. Liu, Commun. Comput. Phys. **2**, 451 (2007).
[22] G. Kresse and J. Hafner, Phys. Rev. B **47**, 558 (1993).
[23] J. P. Perdew and A. Zunger, Phys. Rev. B **23**, 5048 (1981).
[24] P. E. Blöchl, Phys. Rev. B **50**, 17953 (1994).
[25] P. Chandrachud, B. S. Pujari, S. Haldar, B. Sanya, and D. G. Kanhere, J. Phys.: Condens. Matter **22**, 465502 (2010).
[26] M. Z. S. Flores, P. A. S. Autreto, S. B. Legoas, and D. S. Galvao, Nanotech. **20**, 465704 (2009).
[27] L. A. Chernozatonskii and P. B. Sorokin, J. Phys. Chem. C **114**, 3225 (2010).
[28] P. Ruffieux *et al.*, Phys. Rev. B **66**, 245416 (2002).
[29] D. Yu and F. Liu, Nano Lett. **7**, 3046 (2007).
[30] L. Sun, Q. Li, H. Ren, H. Su, Q. W. Shi, and J. Yang, J. Chem. Phys. **129**, 074704 (2008).
[31] W. Bao *et al.*, Nat. Nanotech. **4**, 562 (2009).